# An efficient ICT-based ratio/colorimetric tripodal azobenzene probe for the recognition/discrimination of $F^-$, $AcO^-$ and $H_2PO_4^-$ anions†

Xian Liao,[a] Jun-An Fang,[a] Jiang-Lin Zhao,*[b] Qin Ruan,[a] Xi Zeng,*[a] Qingying Luo*[b] and Carl Redshaw[c]

[a] Key Laboratory of Macrocyclic and Supramolecular Chemistry of Guizhou Province; School of Chemistry and Chemical engineering, Guizhou University, Guiyang 550025, China. E-mail: zengxi1962@163.com (X. Zeng)

[b] Institute of Biomedical & Health Engineering, Shenzhen Institutes of Advanced Technology, Chinese Academy of Sciences, 1068 Xueyuan Avenue, Shenzhen 518055, China. E-mail: zhaojianglin1314@163.com (J.-L. Zhao); qy.luo@siat.ac.cn (Q.Y. Luo)

[c] Dept. of Chemistry & Biochemistry, University of Hull, Hull HU6 7RX, U.K.

The tripodal probe **L** was readily prepared *via* introducing rhodamine and azobenzene groups in a two-step procedure. Studies of the recognition properties indicated that probe **L** exhibited high sensitivity and selectivity towards $F^-$, $AcO^-$ and $H_2PO_4^-$ through a ratiometric colorimetric response with low detection limits of the order of $10^{-7}$ M. The complexation behaviour was fully investigated by spectral titration, $^1H$ NMR spectroscopic titration and mass spectrometry. Probe **L** not only recognizes $F^-$, $AcO^-$ and $H_2PO_4^-$, but can also distinguish between these three anions via the different ratiometric behaviour in their UV-vis spectra (387/505 nm for **L**-$H_2PO_4^-$, 387/530 nm for **L**-$AcO^-$ and 387/575 nm for **L**-$F^-$ complex) or via different colour changes (light coral for **L**-$H_2PO_4^-$, light pink for **L**-$AcO^-$ and violet for the **L**-$F^-$ complex). Additionally, given the presence of NH and OH groups in probe **L**, which can be protonated and deprotonated, probe **L** further exhibited an excellent pH response over a wide pH range (pH 3 to pH 12).

## Introduction

Developing the recognition of anions via the use of artificial probes is of current interest in supramolecular chemistry, given their vital roles in many biological and environmental systems.[1] For example, fluoride ion is useful in the prevention of dental problems and for the treatment of osteoporosis.[2] However, extreme levels of fluoride can cause fluoride toxicity, leading to skeletal fluorosis, nephrotoxic changes, urolithiasis in humans and also contamination can occur in drinking water; the U.S. Environmental Protection Agency (EPA) has set a maximum contaminant level of 4mg/L.[3] Also of interest is the acetate ion, which is an important metabolite in metabolism and cell signaling.[4] Furthermore, in living organisms, phosphorylated species are critical to the storage and transcription of genetic information, energy transduction, and membrane transport.[5] In view of the importance of the $F^-$, $AcO^-$, $H_2PO_4^-$ anions, there is an urgent need to develop suitable probes via a convenient method for the selective detection of these anions.

Many conventional detection methods, including the electrode method and ion chromatography have been developed for the detection of various anions, however, the colorimetric method is emerging as a more promising alternative given its simplicity, high sensitivity, high selectivity, and rapid implementation.[6] The colour change can easily be observed with the naked eye, thus requiring less labor and circumventing the need for advanced instrumentation.[7] In addition,

ratiometric colorimetric probes allow for the measurement of absorption intensities at two different wavelengths, providing a built-in correction for environmental effects and also increasing the dynamic range of absorption measurements possible. This leads to higher accuracy in quantitative determinations,[8,9] and as a consequence, the ratiometric colorimetric method has been employed herein.

Although numerous colorimetric probes have been reported that selectively detect $F^-$[10,11], $AcO^-$[12] or $H_2PO_4^-$,[13] the focus has been mainly on the design of probes with the ability to selectively bind only one specific anion. Reports of single molecular probes that can selectively detect and distinguish between more than two anions are rare. Moreover, the design of multifunctional probes with varying responses towards different analytes is cost effective and convenient for real applications, however the design of probes with multiple analyte recognition capability is a challenging task.

Herein, we introduce a tripodal tris(2-aminoethyl)amine–based colorimetric probe (**L**) which is armed with two azobenzene groups and one rhodamine moiety. The presence of a rhodamine group usually imparts an enhanced response towards $Hg^{2+}$, and similar phenomenon have been observed for probe **L**. However, we will discuss the recognition properties of **L** towards $Hg^{2+}$ elsewhere. In this work, we have focused on the unique properties associated with the azobenzene moiety. In particular, we have employed an electron withdrawing nitro group and an electron-donating hydroxyl group at the azobenzene, which gives rise to a ‘‘push-pull’’ π-electron system for probe **L**. A study of the recognition properties revealed that probe **L** exhibited high selectivity towards $F^-$, $AcO^-$ and $H_2PO_4^-$ *via* intramolecular charge transfer (ICT) and a ratio/colorimetric response. To the best of our knowledge, such multi-functional probes, which are capable of the recognition and discrimination of $F^-$, $AcO^-$ and $H_2PO_4^-$ *via* an ICT mechanism and a ratiometric response are limited in the literature. 14a

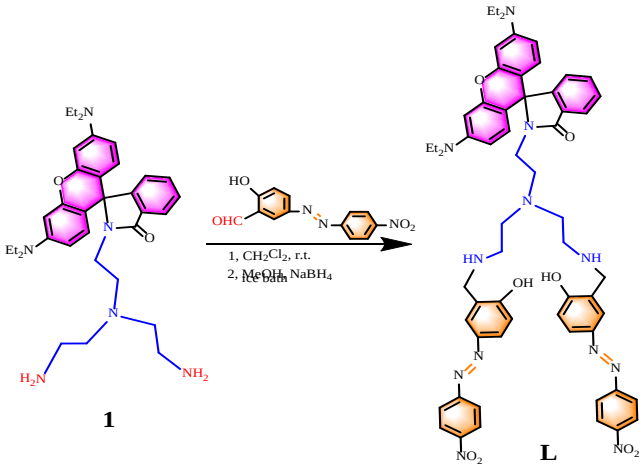


**Scheme 1** The synthetic route to probe **L.**

## Results and discussion

### Synthesis

Compound **1** was previously obtained in a reasonable yield but on a small scale (mg) as reported by kaewtong *et al.*[15] We have further optimized this reaction on a larger scale (g) and in a higher yield (87%). Thanks to the facile preparation and numerous possibilities for the functionalization of compound **1**, there are many possible avenues to explore.[11,16] In view of the high importance of anion recognition and the interesting properties of azobenzene compounds,[17] we have introduced the (*E*)-2-hydroxy-5-((4-nitrophenyl)diazenyl)benzaldehyde group to compound **1** and constructed a tripodal structure. Schiff base groups can be unstable for certain applications, so. we have further

treated the system with $NaBH_4$ to afford the reduced product probe **L** bearing extra anion binding sites, namely NH groups. The structure of **L** was fully elucidated by $^1H$ and $^{13}C$ NMR spectroscopy as well as by mass spectrometry (Figs. S1-S3).

**Recognition properties of probe L towards anions**

The recognition properties of probe **L** were investigated by UV-Vis absorption spectra. It is well-known that hydrogen bonding interactions of anions with a host molecule generally diminish in protic solvents. Hence, most of the anion recognition processes were observed in non-aqueous and aprotic solvents. Herein, we investigated the effect of anions towards probe **L** (10 μM ) in $CH_3CN$ solution. The absorption spectra of probe **L** exhibited solvatochromism. As depicted in Fig. S4 and Table S1**,** the absorption wavelength was red-shifted on increasing the solvent polarity, implying that the absorption originated from the ICT state.[19] As shown in Fig. 1 & Fig. S5, probe **L** exhibited a light orange colour with an intense absorption band at wavelength 274 nm ($\varepsilon = 5.0 \times 10^4\ M^{-1}\ cm^{-1}$) and a lower-energy band with a peak at 387 nm ($\varepsilon = 4.3 \times 10^4\ M^{-1}\ cm^{-1}$). These bands can be assigned respectively to a $\pi \rightarrow \pi^*$ transition and an intramolecular charge transfer (ICT) band from the hydroxyl group to the nitro group. [17,18,20]

Upon addition of the $H_2PO_4^-$ anion, the absorption band at 387 nm decreased greatly and a new absorption band appeared at 505 nm (Fig. 1). While in the presence of the $AcO^-$ anion, the absorption band at 387 nm decreased slightly, but with a greater red shift absorption to 530 nm. More surprisingly, upon the addition of $F^-$, the original max absorption peak at 387 nm almost disappeared and an acute absorption band was observed at 575 nm. The different ratiometric response maybe ascribed to the different steric structures of the $F^-$ (spherical), $AcO^-$ (Y-shaped) and $H_2PO_4^-$ (tetrahedral) anions, which resulted in different interactions. The different absorption bands resulted in obvious colour changes (from light orange to light coral ($H_2PO_4^-$), light pink ($AcO^-$) and violet ($F^-$)), which means that we can directly detect these three anions by the naked eye. The visible colour changes are mainly because of the detection of anions by the receptor molecules through hydrogen bonding.[21] On the other hand, no significant signal changes can be observed in the presence of any other anions ($Cl^-$, $Br^-$, $I^-$, $NO_3^-$, $HSO4^-$, $PF_6^-$) indicating the high selectivity of probe **L**.

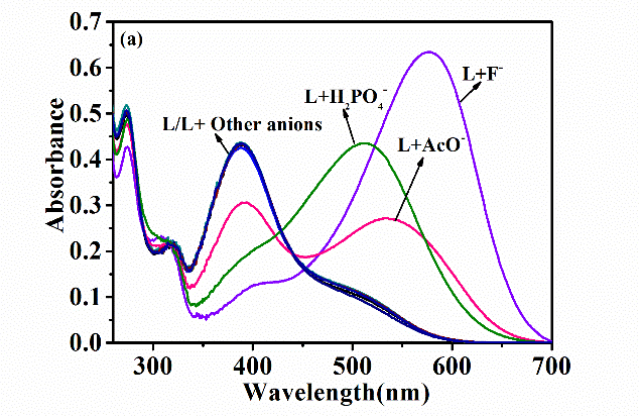


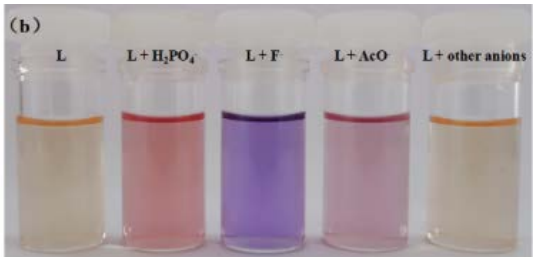

**Figure 1.** (a) Absorption spectra of probe **L** (10 μM, $CH_3CN$) with or without 20 equiv. of the various anions. (b) The colour changes of the probe **L** in the absence and the presence of $H_2PO_4^-$, $F^-$ or $AcO^-$ under sunlight. Other anions include $Cl^-$, $Br^-$, $I^-$, $NO_3^-$, $HSO4^-$, $PF_6^-$.

In order to investigate the detailed recognition processes, absorption titration experiments were carried out. Upon increasing the concentration of $H_2PO_4^-$, the absorption at 387 nm gradually decreased, whilst the absorption at 505nm dramatically increased with an isobestic point at 425 nm (Fig. 2a). The ratiometric absorption change indicated that probe **L** can serve as a ratiometric probe for $H_2PO_4^-$. It is well-known that ratiometric response probes are better than any of other type of probe given their built-in correction for environmental effects and self-correcting capability.[9,22] Similar phenomena can be observed upon the addition of $AcO^-$ (Fig. 2b) and $F^-$ (Fig. 2c) except for the degree of the ratiometric change and red shift. The presence of the $AcO^-$ anion only resulted in a limited ratiometric change at 387/530 nm. However, increasing the $F^-$ anion concentration resulted in a dramatic ratiometric change at 387/575 nm. It should be noted that the degree of red shift is obviously different, *viz* 387 nm red shifted to 505 nm (@$H_2PO_4^-$), 530 nm (@$AcO^-$) and 575 nm (@$F^-$) which results in the different colour changes (Fig. 1b), and enabled us to discriminate between them. This behavior is attributed to the differing complexation ability and binding modes of probe **L** towards the different steric structures and the size of guests. According to the molar ratio method, equilibrium was reached upon addition of about 2.0 equivalent of $H_2PO_4^-$ or $AcO^-$ or $F^-$, which suggested a 1:2 complex stoichiometry for these complexes (Fig. S6).

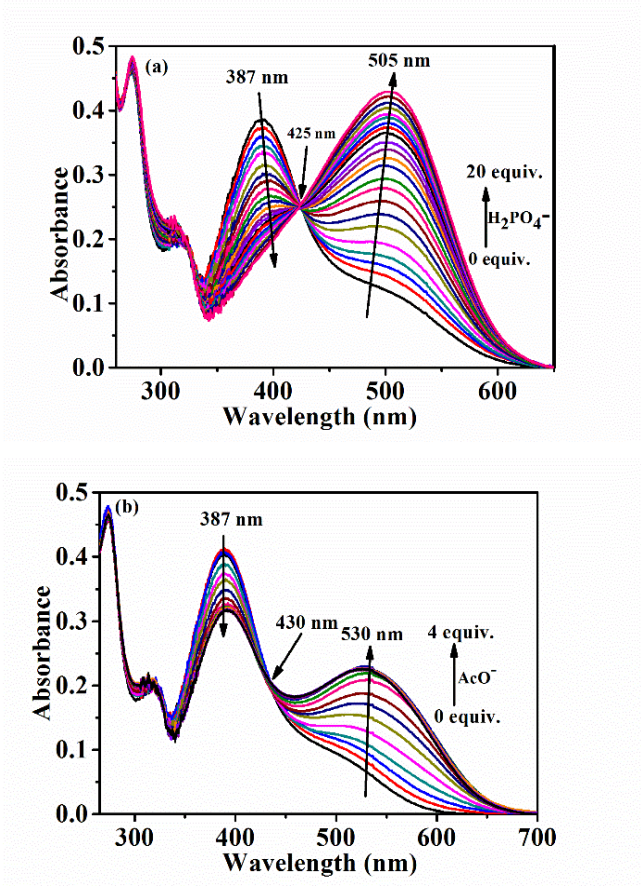

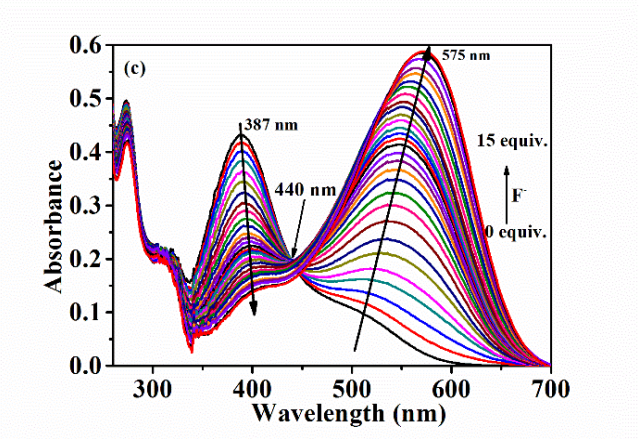


**Figure 2.** Absorption spectral changes of probe **L** (10 μM, $CH_3CN$) solution upon addition of (a) $H_2PO_4^-$ (0 ~ 20 equiv.); (b) $AcO^-$ (0 ~ 4 equiv.); (c) $F^-$ (0 ~ 15 equiv.).

The practical applicability of probe **L** (10 μM) as a selective ratio/colormetric probe for the $F^-$ or $AcO^-$ or $H_2PO_4^-$ anions has been investigated using the UV-vis method. For example, in the presence of $F^-$ mixed with 20 equiv. of other interferential anions $Cl^-$, $Br^-$, $I^-$, $NO_3^-$, $ClO_4^-$, $HSO_4^-$, $PF_6^-$, $AcO^-$ and $H_2PO_4^-$ in $CH_3CN$ solution, no significant interference was observed except for $AcO^-$ or $H_2PO_4^-$ (Fig. 3). However, as mentioned previously, we can further discriminate these three anions based on their different max absorption peak (505 nm/ 530 nm/ 575nm). In other words, the presence of these three anions did not interfere with the detection of each of them individually. Similar phenomena have been observed for the co-existing experiments of $AcO^-$ and $H_2PO_4^-$ (Fig. S7), *viz* probe **L** exhibited a high selectivity towards these three anions. Consequently, this data suggests that probe **L** can serve as a selective probe for $H_2PO_4^-$, $AcO^-$ or $F^-$ in the presence of the above mentioned anions in real life applications.

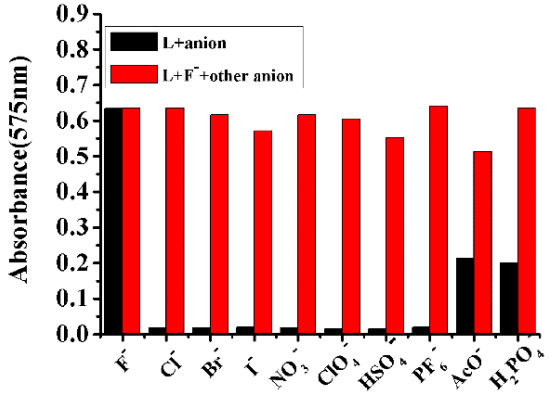


**Figure 3.** Absorption response of probe **L** + $F^-$ with competing anions. Black bars: The absorbance of probe **L** at 575 nm on addition of the respective anions (20 equiv.). Red bars: The absorbance of **L** + $F^-$ complex on addition of the respective competing anions (20 equiv.).

Under optimal conditions, the detection of linear relationships and limits of detection of probe **L** for $F^-$, $AcO^-$ or $H_2PO_4^-$ are summarized in Table 1. The detection limit (LOD = 3σ /slope, Fig. S8) of probe **L** towards $F^-$, $AcO^-$ or $H_2PO_4^-$ were calculated to be of the order of $10^{-7}$ M. These results strongly suggest that the probe **L** is a sensitive multi-functional probe for the detection of $F^-$, $AcO^-$ or $H_2PO_4^-$. The association constants ($K_a$) for **L**+$F^-$, **L**+$AcO^-$ or **L**+$H_2PO_4^-$ complexes were calculated by nonlinear fitting according to the method of Thodarson (Fig. S9).[23] The high association constants suggested that the **L**+$F^-$ or **L**+$AcO^-$ or **L**+$H_2PO_4^-$ complexes were very stable.

**Table 1** Analysis parameters for probe **L** and detection of $F^-$, $AcO^-$ or $H_2PO_4^-$.

| Anions ($\lambda_{max}$) | The linear range of the calibration curve (μM) | Correlation coefficient | LOD ($\times 10^{-7}$ M) | Association constants $K_a$ |
|---|---|---|---|---|

| | | | | |
|---|---|---|---|---|
| $F^-$ (575 nm) | 1.0 ~ 20 | 0.9987 | 4.65 | $K_1$ = 912.0 $K_2$ = 3.382 × $10^6$ |
| $AcO^-$ (530 nm) | 1.0 ~ 20 | 0.9899 | 9.77 | $K_1$ = 93.83 $K_2$ = 2.964 × $10^7$ |
| $H_2PO_4^-$ (505 nm) | 1.0 ~ 20 | 0.9976 | 8.29 | $K_1$ = 632.7 $K_2$ = 1.559 × $10^6$ |

**Optical response of probe L towards pH**

The pH-dependent absorption characteristics of probe **L** (10 μM) were evaluated. As expected, probe **L** can operate as a sensor over a wide pH range, namely from pH 3 to pH 12 (Fig. 4). The pH response process seems be divided into two parts (Fig. S10). When the pH value was increased from pH 3 to pH 10, the max absorption band of probe **L** (387 nm) gradually diminished and then disappeared. Furthermore, a new peak appeared which gradually enhanced and was accompanied by a large red shift (from 500 nm to 550 nm, Fig. 4a). On continuously increasing the pH from 10 to 12, only the max absorption band underwent a further red shift to 595 nm (Fig. 4c). Good linearity ($R^2$ = 0.9947) can be observed for both of these two processes (pH 3 ~ 10 & pH 11 ~ 12, Fig. S11& S12) which means probe **L** can be used to accurately measure pH values from pH 3 ~ 12. In particular, for the process at pH 11~12, probe **L** can further serve as a precise pH sensor based on the big absorption intensity change over a small pH range (only 1).

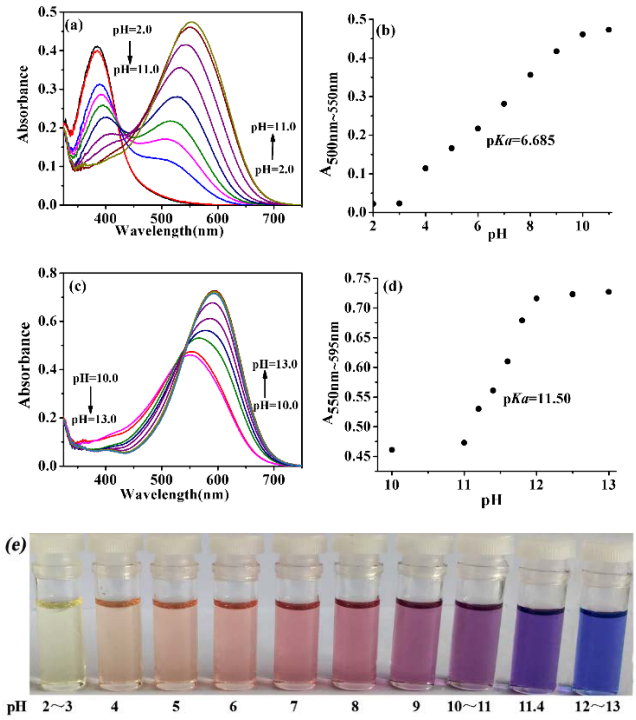


**Figure 4.**(a) Absorption spectra of probe **L** (10 μM, DMSO/$H_2O$, 95/5, v/v) at different pH values (pH = 2.0 ~ 11.0); (b, d) The plot of max absorbance intensity of probe **L** as a function of different pH;(c) Absorption spectra of probe **L** (10 μM, DMSO/$H_2O$, 95/5, v/v) at different pH values (pH = 10.0 ~ 13.0); (e) Colour changes of probe **L** (10 μM, DMSO/$H_2O$, 95/5, v/v) at different pH under sunlight.

Obvious colour changes are observed for probe **L** in solution, where on gradually increasing the pH value from pH 2 to pH 13, the colour changes from light yellow to pink and then to violet (Fig.

4e). These distinct colour changes are attributed to the changes in the maximum wavelength of probe **L** in the absorption spectra. Inspired by these colour changes, we further explored probe **L** as a "naked-eye" indicator of pH from pH 3 to pH 12. A pH test strip was prepared by dip coating a solution of probe **L** onto a filter paper and then subsequently drying in air. The colour of the test strips immediately changed as the newly prepared pH test strips were immersed in solutions of different pH (Fig. 5).

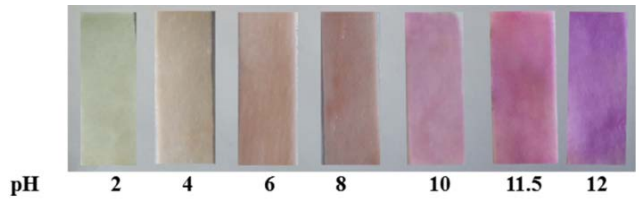


**Figure 5.** Photographs of the colour change of probe **L** on test strips after contact with various pH values (pH = 2, 4, 6, 8, 10, 11.5, 12) under sunlight.

### The recognition mechanism of probe L towards $F^-$, $AcO^-$ and $H_2PO_4^-$anions

In order to understanding the recognition mechanism of probe **L** towards $F^-$, $AcO^-$ and $H_2PO_4^-$, $^1H$ NMR titration experiments have been carried out in DMSO-$d_6$ using the TBA salts of the $F^-$, $AcO^-$ and $H_2PO_4^-$ anions (given the limited solubility of probe **L** in $CH_3CN$, studies cannot be conducted in $CH_3CN$ solution). Upon increasing the concentration of $F^-$, the chemical shifts of the azobenzene moiety were shifted up-field (Fig.6a), especially the protons $H_5$ and $H_2$ adjacent to the phenol OH, $\triangle\delta$ = 0.13 & 0.16 ppm respectively. Moreover, the proton $H_1$ which is adjacent to the imine *NH* group also exhibited a large up-field shift ($\triangle\delta$ = 0.21 ppm). No obvious chemical shift changes have been observed for the other protons, and these results favor the presence of H-bonding between the -NH and -OH groups of probe **L** and $F^-$. The peaks for the NH & OH groups were greatly decreased in the IR spectra, which further confirmed that the NH & OH were participating in the complexation (Fig. S15a). The observed significant red shift in the photophysical behavior and above observations for probe **L** upon interaction with anions is attributed to the enhanced intramolecular charge transfer encountered on formation of the hydrogen bonding followed deprotonation of -NH, -OH fragments.[24] In addition, we note that after the addition of two equivalents of $F^-$ ion, the complex reached an equilibrium, which suggested a 1:2 stoichiometry for the probe-fluoride interaction. This 1:2 stoichiometry was unambiguously confirmed by HRMS mass spectrometry (complex $[\mathbf{L}+2F]^-$ *m/z* 1118.3157, Fig. 6b). The possible binding model for the probe **L** with $F^-$ ion is shown in Fig. 6c. Similar phenomena have been observed in the presence of $AcO^-$ and $H_2PO_4^-$ by $^1H$ NMR spectroscopic titrations, IR spectroscopy and mass spectrometry (Fig. S13~S15), and suggests a similar binding model for them. The only difference between these anions is the slight chemical shift changes, which may be attributed to the different steric structures and sizes of the $F^-$ (spherical), $AcO^-$ (Y-shaped) and $H_2PO_4^-$ (tetrahedral) anions.

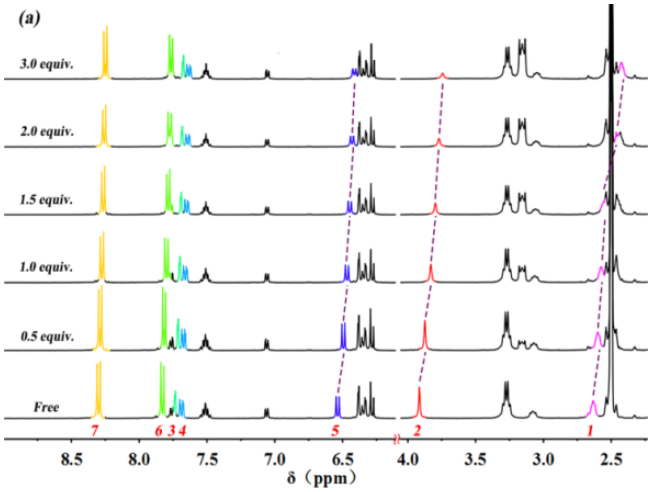

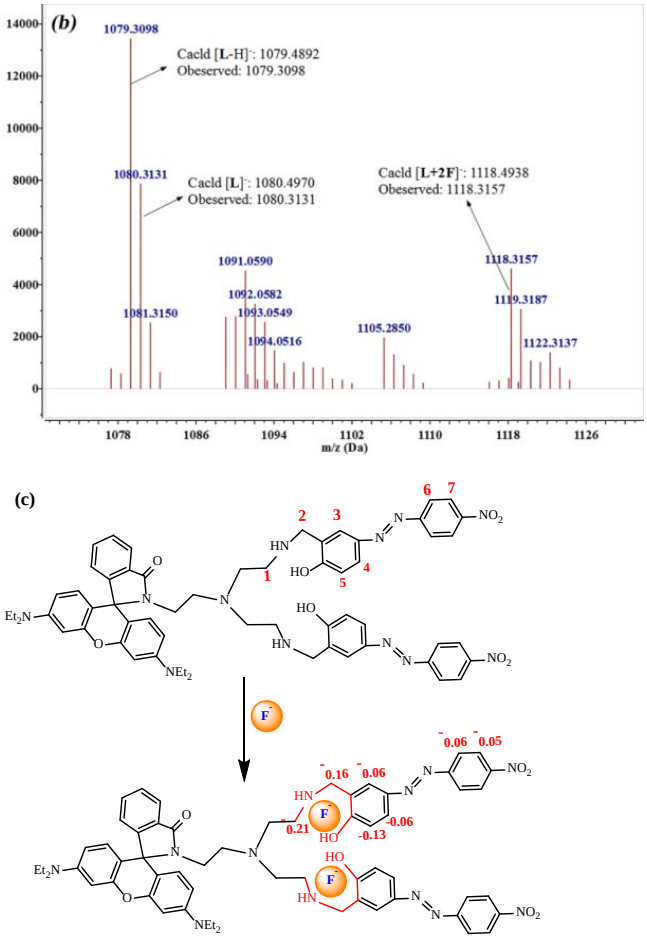


**Figure 6**. (a) Partial $^{1}$H NMR spectra of probe **L** and increasing concentrations of $F^-$ in DMSO-$d_6$ at 298 K; (b) The HRMS spectra of **L**-$F^-$ complex; (c) Plausible recognition mechanism of the probe **L** towards $F^-$. − denotes an up-field shift.

## Conclusions

In summary, a multifunctional/colormetric tripodal probe **L** has been conveniently armed with azobenzene and rhodamine groups. The probe **L** exhibited a high selectivity and sensitive recognition for the anions $F^-$, $AcO^-$ and $H_2PO_4^-$ with ratio/colorimetric behaviour. Due to the different ratiometric response behaviour, probe **L** can further discriminated between these three anions. Furthermore, the probe contains multiple *NH* and *OH* groups, which can be protonated and deprotonated. Probe **L** exhibited an excellent pH response over a wide range from pH 3 to pH 12. These responses induced obvious colour changes, which enabled us to readily detect the anions $F^-$, $AcO^-$ and $H_2PO_4^-$ by the naked eye and conveniently monitor the pH via test strips over a wide pH range.

## Experimental

### Materials and equipment

All solvents used were dried and distilled by standard procedures prior to use. Unless otherwise stated, all reagents used were purchased from commercial sources and were used without further purification. All the anions used were tetra-*n*-butylammonium salts (Sigma-Aldrich Chemical Co., Ltd.), and were stored in a desiccator under vacuum containing self-indicating silica. Double distilled water was used throughout. Compound **1** was prepared by following the reported procedures.[11,16]

UV-Vis absorption spectra were conducted on a UV-1800 spectrophotometer (Shimadzu) in a 1 cm quartz cell. $^{1}$H and $^{13}$C NMR spectra were measured on a JEOL JNM-ECZ400S 400 MHz NMR

spectrometer (JEOL) at room temperature using TMS as an internal standard. MALDI-TOF mass spectra were measured on an AB SCIEX TripleTOF$^{AM\ 5600}$ system. Microelectrode layers used the sputtering and lift-off process with the standard photo-lithography (EVG 610, Austria). Various pH solutions were measured using a pH meter (Orion). Melting points are uncorrected.

**Synthesis of probe L**

A mixture of compound **1** (570 mg, 1 mol) and (*E*)-2-hydroxy-5-((4-nitrophenyl)diazenyl)benzaldehyde (740 mg, 4.00 mmol) in dry $CH_2Cl_2$ (50 mL) was reacted at room temperature under an $N_2$ atmosphere. After 12h, 10 mL dry methanol solvent was added followed by 320 mg $NaBH_4$ in batches. The mixture was reacted for another 5 h., after which the solvent was removed by evaporation. The residue was extracted with $CHCl_3$ (60 mL) three times, washed with water and dried with anhydrous $MgSO_4$. The $CHCl_3$ solvent was removed by evaporation to afford a crimson oil product. The crude product was further purified by silica gel chromatography using $CH_2Cl_2$/MeOH/$NEt_3$ (100/2/1, v/v/v) as eluent to give 470 mg of a crimson solid **L** in 43.4 % yield. m.p. 147.3 ~ 148.5°C. $^1$H NMR (400 MHz, $CDCl_3$, ppm) δ: 8.34 (d, *J* = 8.8 Hz, 4 H, ArH), 7.94 (d, *J* = 8.8 Hz, 4 H, ArH), 7.84 ~ 7.82 (m, 3 H, ArH), 7.70 (s, 2 H, ArH), 7.52 ~ 7.44 (m, 2 H, ArH), 7.14 (d, *J* = 6.8 Hz, 1 H, ArH), 6.86 (d, *J* = 8.8 Hz, 2 H, ArH), 6.43 ~ 6.41 (m, 4 H, ArH), 6.30 (dd, *J* = 8.8 Hz, 2.5 Hz, 2 H, ArH), 4.08 (s, 4 H, Ar*CH*$_2$NH × 2), 3.32 (q, *J* = 7.0 Hz, 8 H, *CH*$_2$$CH_3$ × 4), 3.16 (t, *J* = 7.0 Hz, 2 H, Rhd-N*CH*$_2$$CH_2$), 2.62 ~ 2.52 (m, 8 H, $NCH_2CH_2$-), 2.23 (t, *J* = 7.6 Hz, 2 H, $NCH_2CH_2$), 1.14 (t, J = 7.0 Hz, 12 H, -$CH_2$*CH*$_3$ × 4). $^{13}$C NMR (100 MHz, $CDCl_3$) δ 12.66, 29.80, 38.63, 44.47, 45.90, 51.93, 53.82, 65.51, 97.97, 105.50, 108.30, 117.48, 122.65, 122.84, 122.95, 123.97, 124.06, 126.16, 128.50, 129.10, 131.54, 132.75, 145.48, 147.97, 149.00, 152.77, 153.70, 156.30, 164.39, 168.21 ppm. ESI-HRMS Calcd for [$C_{60}H_{65}N_{12}O_8$]: *m/z* 1081.5048, Found: *m/z* 1081.4923[M+H]$^+$.

**Spectral measurements**

The pH-dependent spectral characteristics of probe **L** were investigated by absorption spectroscopy in different media. To a 10 mL volumetric flask containing various pH solutions, for pH from 2 to 10, diluted with DMSO and Tris-HCl (10 mM) buffers to 10 mL; for pH from 11 to 13 diluted with DMSO and HEPES-NaOH (10 mM) buffers to 10 mL. All samples in experiments were performed in DMSO/Tris or HEPES (v/v, 95/5) buffer aqueous solution and the pH value was confirmed by use of a pH meter.

The recognition properties of probe **L** toward various ions were investigated by absorption spectroscopy in different media. To a 10 mL volumetric flask containing different ions, the $F^-$, $AcO^-$ and $H_2PO_4^-$ was added and this was diluted with $CH_3CN$ to 10 mL, then the absorption sensing of the ions was conducted. Absorption spectroscopy were measured after 0 min upon addition of ions at room temperature to equilibrium.

## Acknowledgements

This work was supported by the “Chun-Hui” Fund of Chinese Ministry of Education (Z2016008), the Basic Research Program of Shenzhen (JCYJ20170818161714678, JCYJ20170413153034718 & JCYJ20170818164040422), the SIAT Innovation Program for Excellent Young Researchers (2017014), the Natural Science Foundation of China (No.21505150), the Major Program of Guangdong Science and Technology Project (2016B020238003) and Shenzhen Peacock Plan. CR thanks the EPSRC for an Overseas Travel grant.

## Notes and references

1 (*a*) M. H. Lee, J. S. Kim and J. L. Sessler, *Chem. Soc. Rev.*, 2015, **44**, 4185-4191; (*b*) D. Wu, A. C. Sedgwick, T. Gunnlaugsson, E. U. Akkaya, J. Yoon and T. D. James, *Chem. Soc. Rev.*, 2017, **46**, 7105-7123; (*c*) Y. Yu, Q. Zhang, Y, Wang, D. K. Galanakis, K. Levon, M, Rafailovich, *Analyst*, 2016, **141**, 5607-5617; (*d*) Y. Yu, Q. Zhang, J. M. Buscaglia, Y, Wang, Y. Liu, K. Levon, M, Rafailovich, *Analyst*, 2016, **141**, 4424-4431.

2 (*a*) S. Ayoob and A. K. Gupta, *Crit. Rev. Environ. Sci. Technol.*, 2006, **36**, 433–487; (*b*) M. Cametti and K. Rissanen, *Chem. Commun.*, 2009, 2809–2829.

3 (*a*) S.Y. Kim, J. Park, M. Koh, S.B. Park and J.-I. Hong, *Chem. Commun.*, 2009, 4735–4737; (*b*) P. P. Singh, M. K. Barjatiya, S. Dhing, R. Bhatnagar, S. Kothari and V. Dhar, *Urol. Res.*, 2001, **29**, 238–244; (*c*) P. Razdan, B. Patthi, J. K. Kumar, M. Prasad, N. Agnihotri and P. Chaudhari, *J. Int. Soc. Prev. Community Dent.*, 2017, **7**, 252-258; (*d*) Z. Li, B. Yang, S. Sekine, S. Zhuang, D. Zhang, Y. Yamaguchi, *Sens. Actuators, B*, 2018, **265**, 110-114.

4 B. Qiu, B. Xia, Q. Zhou, Y. Lu, M. He, K. Hasegawa, Z. Ma, F. Zhang, L. Gu, Q. Mao, F. Wang, S. Zhao, Z. Gao and J. Liao, *Cell Res*., 2018, **28**, 644-654.
5 J. L. Sessler, P. A. Gale, W. -S. Cho, Anion Receptor Chemistry; The Royal Society of Chemistry: Cambridge, 2006.
6 (*a*)X. Xu, M. Wei, Y. Liu, X. Liu, W. Wei, Y, Zhang and S. Liu, *Biosens. Bioelectron*., 2017, **87**, 600-606; (*b*) B. Liu, Z. Wang, L. Lan, Q. Yang, P. Zhang, L. Shi, Y. Lang, A. Tabib-Salazar, S. Wigneshweraraj, J. Zhang, Y. Wang, Y. Tang, S. Matthews and X. Zhang, *Chem-Eur. J.*, 2018, **24**, 6727-6731; (*c*) Ding, W. H. Zhu and Y. Xie, *Chem. Rev*., 2017, **117**, 2203–2256.
7 (*a*) B. Kaur, N. Kaur and S. Kumar, *Coord. Chem. Rev*., 2018, **358**, 13-69; (*b*) S. Lee, J. Li, X. Zhou, J. Yin and J. Yoon, *Coord. Chem. Rev*., 2018, **366**, 29-68.
8 (*a*)W. Feng, J. Hong and G. Feng, *Sens. Actuators, B*, 2017, **251**, 389-395; (*b*) H. Zhu, J. Fan, B. Wang and X. Peng, *Chem. Soc. Rev*., 2015, **44**, 4337-4366.
9 J.-L. Zhao, H. Tomiyasu, C. Wu, H. Cong, X. Zeng, S. Rahman, P. E. Georghiou, D. L. Hughes, C. Redshaw and T. Yamato, *Tetrahedron*., 2015, **71**, 8521-8527.
10 (*a*) Y. Fu, C. Fan, G. Liu and S. Pu, *Sens. Actuators, B*, 2017, **239**, 295-303; (*b*) Y.-C. Wu, J.-Y. You, K. Jiang, J.-C. Xie, S.-L. Li, D. Cao and Z.-Y. Wang, *Dyes Pigm*., 2017, **140**, 47-55; (*c*) H. Zhang, T. Sune, Q. Ruana, J.-L. Zhao, L. Mu, X. Zeng, Z. Jin, S. Su , Q. Luo, Y. Yan and C. Redshaw, *Dyes Pigm.*, 2019, **162**, 257–265; (*d*) T. G. Jo, Y. J. Na, J. J. Lee, M. M. Lee, S. Y. Lee and C. Kim, *New. J. Chem*., 2015, **39**, 2580-2587; (*e*) Z. Li, J. Huang, B. Yang, Q. You, S. Sekine, D. Zhang, Y. Yamaguchi, *Sens. Actuators, B*, 2018, **254**, 153-158
11 Q. Ruan, L. Mu, X. Zeng, J.-L. Zhao, L. Zeng, Z.-M. Chen, C Yang, G. Wei and C. Redshaw, *Dalton Trans*., 2018, **47**, 3674–3678.
12 (*a*) V. K. Gupta, A. K. Singh, S. Bhardwaj and K. R. Bandi, *Sens. Actuators, B*, 2014, **197**, 264-273; (*b*) Y. Jiang, L.-L. Sun, G.-Z. Ren, X. Niu and Z.-Q. Hu, *Talanta.*, 2016, **146**,732-736; (*c*) X. Shang, J. Li, K. Guo, Q. Dang, T. Wang, J. Zhang and X. Xu, *Curr. Org. Synth*., 2018, **15**, 143-149; (*d*) A. Singh, S. Tom and D. R. Trived, *J. Photoch. Photobio. A*., 2018, **353**, 507-520.
13 (*a*) R. Hu, G. Long, J. Chen, Y. Yin, Y. Liu, F. Zhu, J. Feng, Y. Mei, R. Wang, H. Xue, D. Tian and H. Li, *Sens. Actuators, B*, 2015, **218**,191-195; (*b*) C. Guo, S. Sun, Q. He, V. M. Lynch and J. L. Sessler, *Org. Lett.*, 2018, **20**, 5414-5417; (*c*) S. Suganya, S. Velmathi, P. Venkatesan, S-P. Wu and M. S. Boobalan, *Inorg. Chem. Front*., 2015, **2**, 649-656.
14 (*a*) J. S. Kim and D. T. Quang, *Chem. Rev*., 2007, **107**, 3780-3799; (*b*) L. E. Santos-Figueroa, M. E. Moragues, E. Climent, A. Agostini, R. Martínez-Máñez and F. Sancenón, *Chem. Soc. Rev*., 2013, **42**, 3489-3613; (c) J.-A. Fang, H. Zhang, L.-F. Zhang, L. Mu, X. Zeng, J.-L. Zhao, G. Wei, *Chinese J. Anal. Chem.*, 2018, **46**, 1739-1747.
15 C. Kaewtong, B. Pulpoka and T. Tuntulani, *Dyes Pigm*., 2015, **123**, 204–211.
16 Z. Li, J. -L. Zhao, Y.-T. Wu. L, Mu. X, Zeng. Z, Jin, G. Wei, N. Xie and C.Redshaw, *Org.Biomol. Chem*., 2017, **15**, 8627–8633.
17 A. A. Beharry and G. A. Woolley, *Chem. Soc. Rev*., 2011, **40**, 4422-4437.
18 D. T. Lien, D. T. M. Huong, L. V. Vu, N. N. Long, *J. Lumin*., 2015, **157**, 383–389.
19 Y. Zhang, S. L. Lai, Q. X. Tong, M. F. Lo, T. W. Ng, M. Y. Chan, Z. C. Wen, J. He, K. S. Jeff, X. L. Tang, W. M. Liu, C. C. Ko, P. F. Wang and C. S. Lee, *Chem. Mater*., 2012, **24**, 61-70.
20 L.-K. Zhang, Q.-X. Tong, and L.-J. Shi, *Dalton Trans*., 2013, **42**, 8567–8570
21 S. Suganya and S. Velmathi, *J. Mol. Recognit*., 2013, **26**, 259-267.
22 (*a*) F. Ghasemi, M. R. Hormozi-Nezhada and M. Mahmoudi, *Sens. Actuators, B*, 2018, **259**, 894–899; (*b*) M. H. Lee, J. S. Kim and J. L. Sessler, *Chem. Soc. Rev*., 2015, **44**, 4185-419.
23 (*a*) P. Thordarson, *Chem. Soc. Rev*., 2011, **40**, 1305-1323; (*b*) D. B. Hibberta and P. Thordarson, *Chem. Commun*., 2016, **52**, 12792-12805.
24 (*a*) R. Ali, S. S. Razi, R. C. Gupta, S. K. Dwivedi and A. Misra, *New J. Chem*., 2016, **40**, 162-170; (*b*) P. Dydio, D. Lichosyt and J. Jurczak, *Chem. Soc. Rev*., 2011, **40**, 2971–2985; (*c*) M. Shahid, P. Srivastava and A. Misra, *New J. Chem*., 2011, **35**, 1690–1700.